J. Micromech. Microeng. **19** (2009) 075009 (9pp) doi:10.1088/0960-1317/19/7/075009

Three-dimensional automated micromanipulation using a nanotip gripper with multi-feedback

Hui Xie and Stéphane Régnier

Institut des Systèmes Intelligents et de Robotique, Université Pierre et Marie Curie/CNRS, 4 Place Jussieu, Paris Cedex, France

E-mail: xie@robot.jussieu.fr

Received 24 February 2009, in final form 11 May 2009
Published 23 June 2009
Online at stacks.iop.org/JMM/19/075009

Abstract

In this paper, three-dimensional (3D) automated micromanipulation at the scale of several micrometers using a nanotip gripper with multi-feedback is presented. The gripper is constructed from protrudent tips of two individually actuated atomic force microscope cantilevers; each cantilever is equipped with an optical lever. A manipulation protocol allows these two cantilevers to form a gripper to pick and place micro-objects without adhesive-force obstacles in air. For grasping, amplitude feedback from the dithering cantilever with its normal resonant frequency is used to search a grasping point by laterally scanning the side of the microspheres. Real-time force sensing is available for monitoring the whole pick-and-place process with pick-up, transport and release steps. For trajectory planning, an algorithm based on the shortest path solution is used to obtained 3D micropatterns with high levels of efficiency. In experiments, 20 microspheres with diameters from 3 μm to 4 μm were manipulated and 5 3D micropyramids with two layers were built. Three-dimensional micromanipulation and microassembly at the scale of several microns to the submicron scale could become feasible through the newly developed 3D micromanipulation system with a nanotip gripper.

(Some figures in this article are in colour only in the electronic version)

1. Introduction

Micromanipulation, as one of significant techniques in the fabrication of three-dimensional (3D) microstructures and in biology applications, has been the subject of investigation for the past decade. Until now, a lot of research effort has focused on building micromechanical or microelectromechanical structures [1–3], fabricating photonic devices [4] and performing scientific explorations in biology [5–9]. For the purpose of building two-dimensional (2D) or 3D microstructures and complete manipulation of biology samples, various end-effectors have been proposed: pushing and pulling with a nanoprobe [10], pick-and-place operations using microgrippers [11–18], a microcantilever [19], collaborating fingers [20] and noncontact tools such as the optical tweezers [21]. In addition, a two-nanotip gripper was first proposed for 3D nanomanipulation as a future work [22].

It is well known that pick-and-place is very important for 3D microstructure fabrication since it is an indispensable step in the bottom-up building process. However, so far, there are few references in the literature that report the mechanical pick-and-place manipulation of micro-objects with feature sizes less than 10 μm, especially manipulation confined in air. The main difficulty in sufficiently completing such pick-and-place manipulation at this scale lies in fabricating a very sharp end-effector that is capable of smoothly releasing micro-objects deposited on the substrate. Moreover, this end-effector has to provide enough grasping force to overcome strong adhesion forces [23–25] from the substrate as well as being capable of sensing and controlling interactions with the micro-objects. Furthermore, compared with the manipulation of larger micro-objects under an optical microscope, visual feedback at several microns more suffers from the shorter depth of focus and the narrower field of view of lenses with high magnifications, although different schemes or algorithms have been introduced

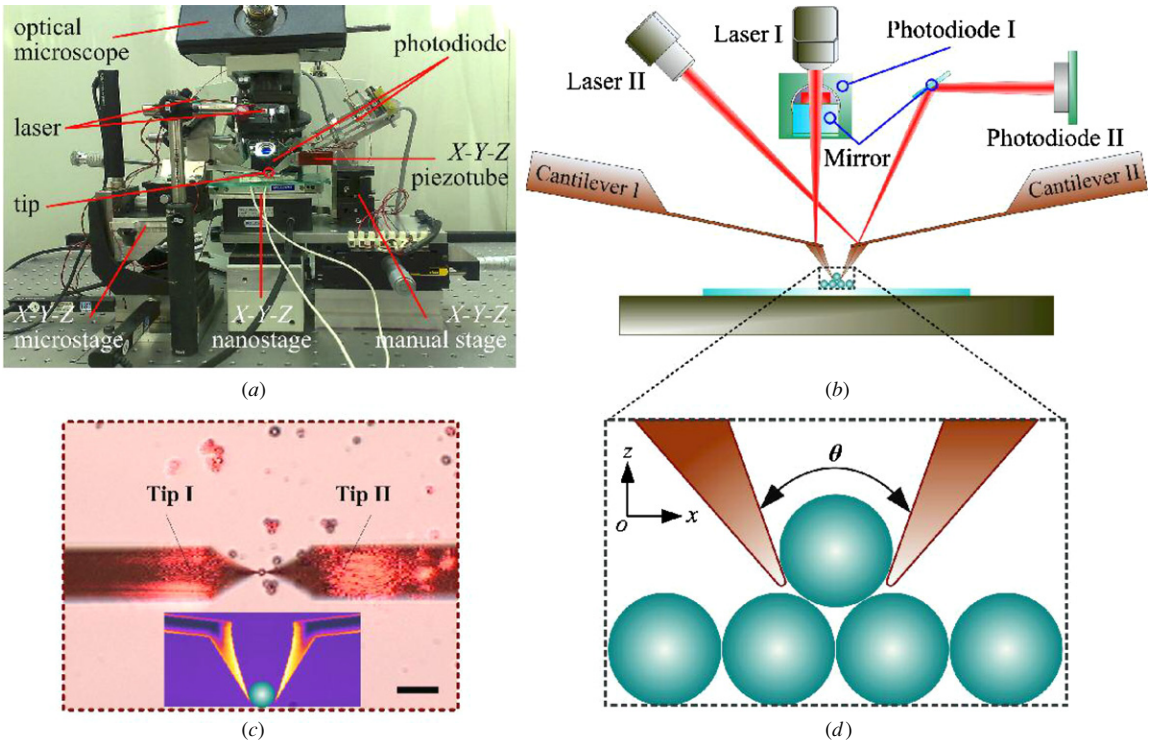

Figure 1. Structure and manipulation schemes of the 3DMS. (*a*) A photo of the developed 3DMS. (*b*) System configuration of the 3DMS, which mainly consists of two sets of devices used in a commercially available AFM, including two cantilevers and the corresponding two sets of nanopositioning devices and optical levers. (*c*) A microscopic image captured during the pick-up operation of a microsphere using the gripper constructed by tip I and tip II. The bottom inset shows a side view of the pick-and-place scheme with a gripper. The scale bar represents 20 μm. (*d*) Close-up figure showing the scheme for grasping a microsphere with the nanotip gripper.

on techniques of autofocusing [26, 27] and extending focus depth [28]. Compared with vision-based automated 2D micromanipulation, automated 3D micromanipulation at the scale of several microns to submicron scale is more challenging because of optical microscope's resolution limit (typically 200 nm). Moreover, additional manipulation feedback is needed, which is beyond the capability of optical vision, such as in the cases of vertical contact detection along the optical axis or manipulation obstructed by opaque components. Therefore, multi-feedback is of vital importance to achieve such accurate and stable 3D micromanipulation at the scale of several microns to submicron scale.

In this paper, in order to achieve the 3D manipulation of micro-objects with feature sizes from submicron to several micrometers, an atomic force microscope (AFM)-based 3D micromanipulation system (3DMS) with a nanotip gripper is developed. The 3DMS mainly consists of two collaborative AFM cantilevers with protrudent tips. The nanotip gripper is constructed from these two tips that can be used to build 2D micropatterns by pushing and pulling micro-objects on a single surface, and more importantly, to achieve 3D microstructures by pick-and-place involving grasp, pick-up, transport and release steps. We have used the 3DMS to fabricate five micropyramids with two layers by manipulating nylon microspheres with diameters of 3 μm–4 μm. Compared with other means of 3D micromanipulation in air, the developed 3DMS is more controllable due to its real-time interactive force sensing and process monitoring.

This paper is organized as follows. Section 2 describes the prototype 3DMS design and presents its experimental setup. Section 3 introduces manipulation schemes for pick-and-place micromanipulation, including methods for grasping point searching and contact detection with amplitude feedback from dithering cantilevers, a 3D manipulation protocol for microspheres and real-time force sensing. In section 4, we show the 3D micromanipulation results of five micropyramids with two layers with each micropyramid being constructed from four microspheres. Section 5 concludes the paper and discusses possible applications of this prototype for the 3D micromanipulation system.

2. System configuration

As shown in figures 1(*a*) and (*b*), the proposed 3DMS is equipped with an optical microscope and two sets of similar devices commonly used in a conventional AFM, mainly including two cantilevers, two sets of nanopositioning devices and optical levers. The optical lever, typically composed of a laser and a quadrant photodiode, is used to detect the actions of each cantilever during micromanipulation. These two optical levers are arranged on two vertical planes due to the space limitation of the optical microscope, as seen in figure 1(*b*). The bottom inset of figure 1(*c*) shows that the nanotip gripper is constructed from two protrudent nanotips of AFM cantilevers I and II that are facing each other. With a mounting angle of 8°, each tip has a tilted angle of about 70° on the side view,

providing the nanotip gripper with a clamping angle of $\theta = 40^\circ$. A typical pick-and-place micromanipulation scheme is depicted in figure 1(*d*), in which the nanotip gripper is used to pick up and place a micro-object in its target position. The 3DMS configuration is described in detail as follows:

(1) Cantilever I, which is immovable during the pick-and-place micromanipulation, is fixed on an *X–Y–Z* micropositioning stage for coarse positioning. The normal spring constant of cantilever I and the sensitivity of its optical lever are calibrated as 2.43 N m^{-1} and 0.65 nm mV^{-1} [29], respectively.
(2) Cantilever II is actuated by an *X–Y–Z* piezotube (PI P-153.10 H) for gripper opening and closing operations. The piezotube has a scan range of 10 μm × 10 μm × 10 μm and a sub-nanometer resolution, which is mounted on an *X–Y–Z* manual microstage. For accurate positioning on tip II, the hysteresis of the piezotube is accurately compensated by the PI operator [30]. The normal spring constant of cantilever II and the sensitivity of its optical lever are calibrated as 2.48 N m^{-1} and 0.58 nm mV^{-1} [29], respectively.
(3) An *X–Y–*Z closed-loop nanostage (MCL Nano-Bio2M on the *X–Y* axes, PI P-732.ZC on the Z-axis), with a maximum motion range of 50 μm × 50 μm × 10 μm and a resolution of 0.1 nm, is used to support and transport samples.
(4) A data acquisition (NI 6289) card with a resolution of 18 bits in A/D transfer and a maximum sampling frequency of 625 kHz is used for high-speed capturing photodiode voltage output to estimate deflections on both cantilevers induced by force loading or resonant oscillation. The acquisition card is also used to actuate the piezotube by exporting voltage signals to three independent amplifiers for each axis.

3. Manipulation schemes

3.1. Overview

The developed 3DMS with the nanotip gripper enables complicated pick-and-place of microspheres (less than 10 μm in diameter) deposited on the substrate. After trajectory planning of a micromanipulation task, the nanotip gripper is used to perform the 3D micromanipulation procedure with contact detection, grasp, transport and release steps for the selected microspheres on expected locations to build a 3D microstructure. Details of manipulation schemes and a manipulation protocol of the 3DMS are discussed as follows.

3.2. Configuration of the two-tip gripper

Configurations of commonly used grippers with two parallel clamping jaws are shown in figures 2(*a*)–(*c*), which are different from the shape of the jaws or roughness of the contact surface. figure 2(*a*) shows the most widely used configuration, and the gripper seen in figure 2(*b*) is designed for holding a micro-object more strongly. In order to decrease adhesion forces between the gripper and the micro-object, a rough contact surface has been proposed [13] and, as shown in figure 2(*c*), a special tip end with tiny contact surface is adopted. Using these three types of commonly used microgrippers, micro-objects with a feature size larger than 10 μm were successfully manipulated in various environments. However, as the size of the micro-object reduces to several microns or submicron, problems will arise with these conventional grippers:

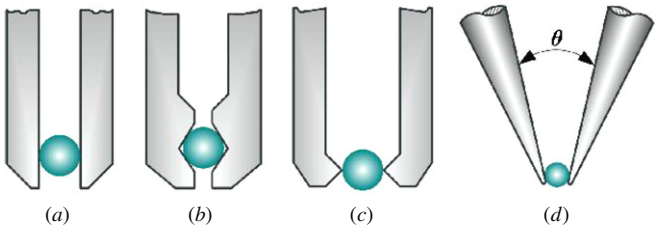

Figure 2. Different types of microgripper configuration. (*a*) The most widely used microgripper which has parallel clamping jaws. (*b*) A gripper with a closed configuration is designed to hold micro-objects more strongly in grasping operation. (*c*) A gripper with a tiny contact area is designed to reduce tip–micro-object adhesion forces. (*b*) A gripper constructed from two AFM tips is adopted in the developed 3DMS.

(1) Sticking phenomena become more severe due to the relatively larger contact area between the gripper and the micro-object [23, 25].
(2) The tip diameters of the clamping jaws are comparable in size to the micro-objects to be grasped. In this case, the clamping jaws are not geometrically sharp enough to pick up smaller micro-objects deposited on the substrate.

Therefore, in order to pick up smaller micro-objects without obstacles, such as the sticking phenomena, and enhance grasping ability to overcome the strong adhesion forces between the micro-object and the substrate, a gripper with a new configuration is proposed in figure 2(*d*). This gripper is constructed from two AFM tips with the following benefits:

(1) The AFM tip end is very tiny (typically around 10 nm in radius) with respect to the size of the micro-object to be manipulated, which leads to smaller adhesive forces because the contact area with the micro-object is much smaller than the micro-object–substrate contact.
(2) However, a smaller contact area also leads to weaker contact friction, which is proportional to the contact area at this scale [31]. In this case, the friction forces of the gripper–micro-object contact, generally used for grasping operations by grippers with parallel clamping jaws, might not be strong enough to break the adhesion forces of the micro-object–substrate contact. Fortunately, for the proposed nanotip gripper, as shown in figure 2(*d*), a positive clamping angle θ is configured making grasping stronger due to the contribution of repulsive forces from the tip–micro-object contact, compounding with the tip–micro-object friction forces to overcome the adhesion forces of the micro-object–substrate contact.

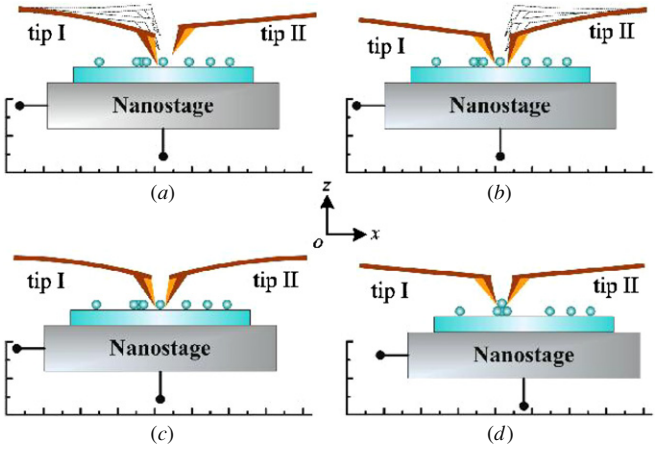

Figure 3. A protocol for the pick-and-place manipulation of microspheres to build a pyramid. Four main steps are involved in a manipulation procedure. The dithering tip I is used to search for the grasping point by local scanning with amplitude feedback in step (*a*). In step (*b*), the grasping point between tip II and the microsphere is detected with the dithering tip II. A nanotip gripper is formed for the grasping operation as both tips make contact with the microsphere. The pick-and-place manipulation is achieved in step (*c*) by moving the nanostage on each axis. (*d*) A micropyramid is achieved as the microsphere is placed on the first microsphere layer.

3.3. Protocol for automated pick-and-place

Microparticles and microspheres are being intensively investigated as significant experimental materials for micromanipulation and microassembly. Thus, one of the 3DMS protocols has been devised for specific applications to the microparticles or microspheres deposited on the substrate. However, the applications of such a protocol can also be extended to include pick- and-place for other types of micro-objects dispersed on the substrate. As shown in figure 3, the pick-and-place procedure mainly includes the following steps.

3.3.1. System initialization. First, each axis of the nanostage and the piezotube are set in a proper position, which will provide the pick-and-place manipulation with enough motion range on each axis.

3.3.2. Task planning. Once the system initialization is ready, task planning is started with image processing of a global view containing all microspheres to be manipulated and the cantilever tips. In our method, the optical microscopy image is just used for coarse positioning of micro-objects and the gripper, providing a distribution of the microspheres for task planning. Subsequently, fine positioning of the microspheres is performed using amplitude or force feedback from the gripper. This will be discussed in section 3.5.

3.3.3. Contact with tip I. Figure 3(*a*) shows that tip I approaches a microsphere to make contact by moving the nanostage on the *X*-axis. A gap (typically 500–800 nm in our experiments) between tip I and the substrate should be kept during the approach to ensure contact with the very end of tip I. The actual grasping point and contact on the microsphere can be detected by the amplitude feedback. Methods for grasping point searching and contact detection will be discussed in section 3.5.

3.3.4. Contact with tip II. Similarly, as in the step depicted in figure 3(*b*), tip II approaches the microsphere by moving the piezotube on the *X*-axis. Once tip II and the microsphere are in contact, in figure 3(*c*), a nanotip gripper is configured for a grasping operation.

3.3.5. Pick-and-place. Once the gripper is constructed, as shown in figure 3(*d*), the microsphere is picked up, transported and placed by moving the nanostage on each axis with a proper displacement that depends on the diameter of the microsphere and its destination. The complete 3D micromanipulation procedure is monitored by the real-time force sensing.

3.4. Task planning

Unlike trajectory planning for 2D pushing/pulling micromanipulation on a singe surface, the blockage problem in trajectory planning can be eliminated in pick-and-place micromanipulation, since the microsphere can be picked up and lifted to a height exceeding that of the micro-objects on the substrate before being transported. An algorithm, for this case, based on the shortest path solution, is proposed for linear trajectory planning on 3D microstructure formations. For the manipulation example shown in figure 4, the task planning is described as follows:

(1) Capture a frame of gray microscopic images.
(2) Detect the central position of each microsphere in the image space using the method adopted in [10].
(3) Determine target positions and manipulation sequences according to the microstructure to be fabricated.
(4) For $n = 1$–N (number of targets) generate all possible linear trajectories between each microsphere and the target position $t_n(x, y)$ in the image space, select the microsphere with a central position $o_n(x, y)$ that has the shortest path to the target position, as shown in figure 4(*a*).
(5) Transform the position sequences $t_n(x, y)/o_n(x, y)$ from the image space into $T_n(x, y)/O_n(x, y)$ nanostage motion space for an actual motion planning of the micromanipulation.

Once the task planning is completed, for each target position, the nanotip gripper is used to pick up and place the nearest microsphere. In this case, amplitude and force feedback on each microcantilever are used to detect grasp, pick-up and place operations instead of commonly used microscopic vision feedback, which will be discussed in the following sections.

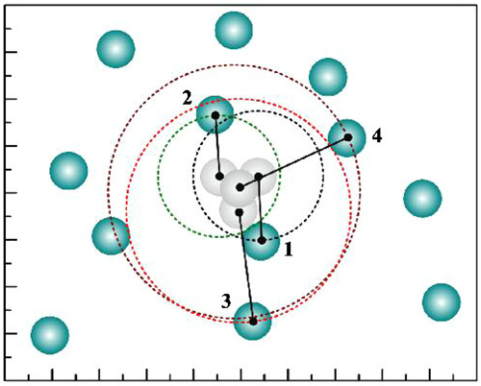

(*a*)

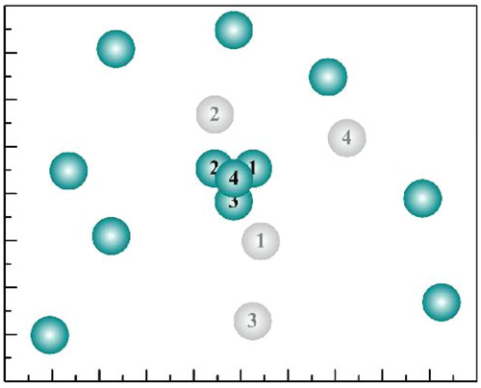

(*b*)

Figure 4. Simulated 3D assembly of a micropyramid constructed from four microspheres using a shortest path algorithm, in which the numbers refer to the order of the manipulation: (*a*) before manipulation, (*b*) after manipulation.

3.5. Grasping point searching and contact detection

In the developed 3DMS, real-time amplitude or force feedback from the gripper is used to detect the interactions between the tip and the micro-object. As shown in figure 5(*a*), the dithering cantilever with the first mode of its natural resonance is utilized to locate grasping points and detect the contact. In order to locate two grasping points distributed over the diameter of the contact circle on the microsphere, as shown in inset I of figure 5(*a*), the dithering cantilever sweeps along the *Y*-axis at a distance about half the microsphere's diameter as it approaches the microsphere. When the tip laterally taps on the microsphere, the grasping point can be accurately located by searching for the minimum amplitude response of each single scan. A corresponding experimental result can be found in figure 5(*b*), in which the tip laterally sweeps the microsphere within a range of 1.6 μm with a free oscillating amplitude of about 320 nm. Six different distances to the microsphere were tested from 120 nm to 20 nm with an interval of 20 nm and, ultimately, the grasping point is well located with an accuracy of $\pm$10 nm, which is greater than that achieved with the optical microscope.

From the scheme depicted in inset II of figure 5(*a*), amplitude feedback is also used for contact detection. In the experimental result shown in figure 5(*c*), contact between the tip and the microsphere is achieved as the amplitude reduces to a steady value close to zero. In addition, contact can also be detected by the normal force response from the gripper. As shown in figure 5(*d*), a full normal force response in an approach-retraction loop can be recognized by snap-in, contact and pull-off steps, usually in the presence of the tip–substrate contact. The interaction responses of the microcantilever described in figures 5(*b*)–(*d*) are sufficient to detect not only the contact between the tip and the micro-object, but also the grasping state. In our experiments, as the contact between tip I and the microsphere is made, tip I retreats 10–20 nm in order to make a tiny gap between tip I and the microsphere. This gap enables smart recognition of the grasping state as being tip II contact with the microsphere after a slight further push. Compared with operations under the optical microscope, the amplitude-detecting method has two obvious advantages:

(1) Grasping points and contact can be detected below the opaque components, more importantly, with a lever of accuracy that is far beyond the capability of the optical microscope.
(2) Benefiting from AFM-based accurate force and amplitude measurement, the grasping points and contact can be successfully detected even with very weak interaction forces at the nano-Newton scale, protecting the fragile tips and the micro-objects from damage during manipulation.

3.6. Force sensing during pick-and-place

In order to measure interactive forces between the gripper and the microsphere in the pick-and-place procedure, as shown in figure 6, during the pick-up operation, the 3D interactive forces on tip I in the defined frame can be measured as a normal signal response from the well-calibrated photodiode using the following equations:

$$F_{z1} = F_{f1}\cos\frac{\theta}{2} + F_{r1}\sin\frac{\theta}{2}, \tag{1}$$

$$F_{x1} = F_{r1}\cos\frac{\theta}{2} - F_{f1}\sin\frac{\theta}{2}, \tag{2}$$

where F_{z1} and F_{x1} are component forces applied on tip I on the *X*-axis and the *Z*-axis in the defined frame, respectively, F_{r1} is the repulsive force and F_{f1} is the friction force, and θ is the clamping angle of the nanotip gripper.

For the sake of calculation convenience, the angular deflection of the cantilever is used because of its linear relation to the voltage output of the optical lever. The bending angular deflection on the free end of the cantilever comprises two parts: ϕ_{z1} and ϕ_{x1}, caused by F_{z1} and F_{x1}, respectively. These two parts can be calculated from

$$\phi_{z1} = \frac{F_{z1}L^2}{2EI}, \tag{3}$$

$$\phi_{x1} = \frac{F_{x1}Ll}{EI}, \tag{4}$$

where L is the effective length of the cantilever, l is the cantilever's tip height, E is Young's modulus of silicon, and I is the moment of inertia on the cantilever's cross section. L, l and θ are measured as 250 μm, 9.5 μm and 40°, respectively. We can estimate $F_{f1} = \mu F_{r1}$ using the assumption $\mu = 0.33$,

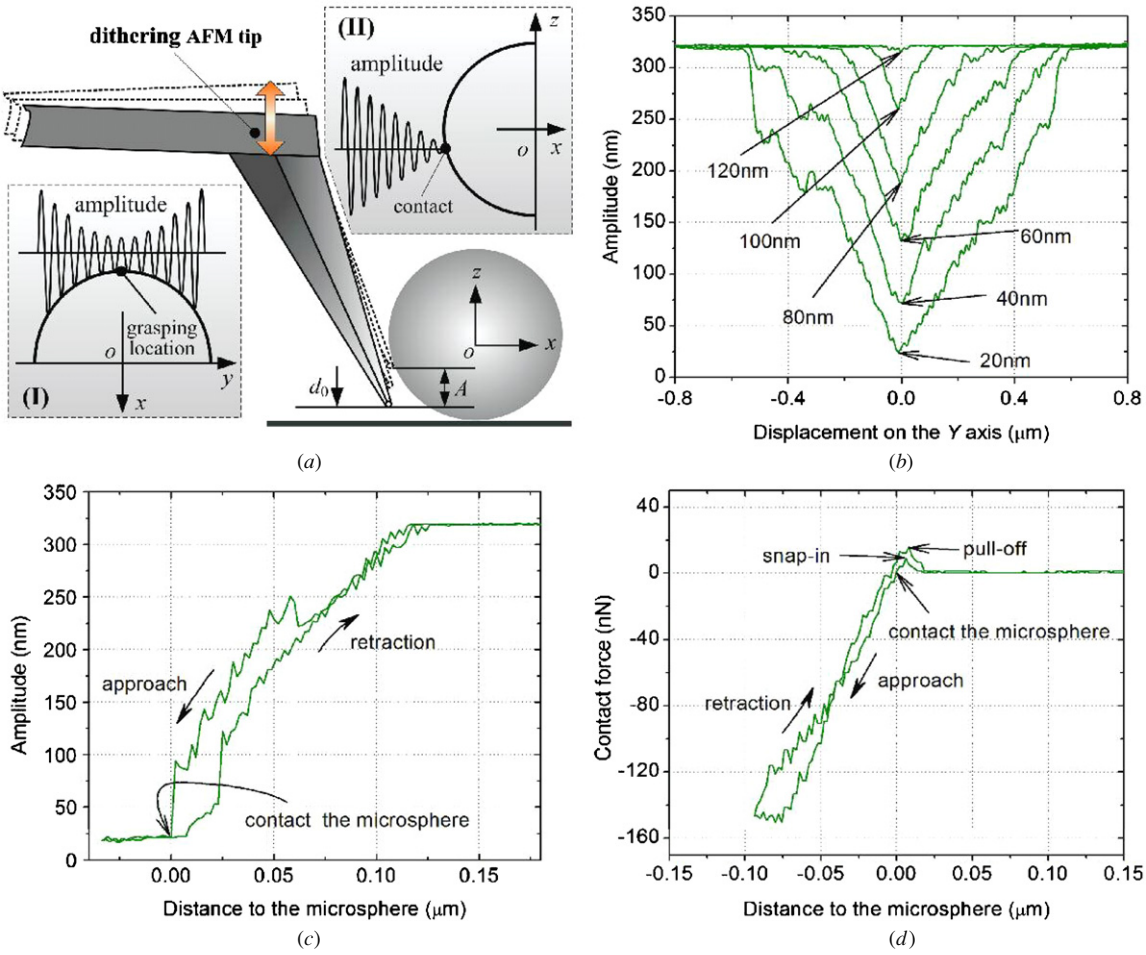

Figure 5. Schemes and experimental results of grasping point searching and contact detection on a microsphere. (*a*) Schematic diagram of grasping point location (inset I) and contact detection (inset II) using the amplitude feedback of a dithering microcantilever with amplitude A. d_0 is the distance between the tip and the substrate. (*b*) Amplitude responses of the microcantilever when it is sweeping along the Y-axis with different distances from the microsphere on the X-axis. Experimental results show that the locating accuracy of the grasping point can be as precise as ± 10 nm. (*c*) Amplitude responses of the cantilever when it is approaching the contact point on the microsphere. (*d*) As an alternative method, normal force responses could also be used for contact detection.

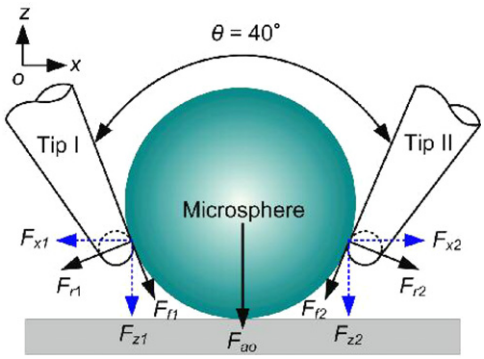

Figure 6. Force simulation of a pick-up operation with the gripper, which has a clamping angle of 40°.

which is one of the experimental values obtained from an AFM lateral force calibration [32]. Assuming the magnitudes of F_{z1} and F_{x1} are in the same order, so from equations (1)–(4), the bending deflection ϕ_{x1} induced from F_{x1} is relatively very small to the bending deflection ϕ_{z1} from F_{z1}. Therefore, to simplify the estimating process of the adhesion force F_{ao} between the microsphere and the substrate, the cantilever deflection caused by F_{x1} will be omitted in the following calculations. Thus, F_{z1} can easily be estimated from the normal voltage output ΔV_1 from the optical lever of tip I from [33]

$$F_{z1} = \beta_1 \cdot \Delta V_1, \tag{5}$$

where β_1 is the normal force sensitivity, and ΔV_1 is the voltage response of the photodiode due to the force loading. A similar result can also be deduced on tip II. Once F_{z1} and F_{z2} are known, the adhesion force F_{ao} can be calculated from

$$F_{ao} = F_{z1} + F_{z2} = \beta_1 \Delta V_1 + \beta_2 \Delta V_2, \tag{6}$$

where β_2 is the normal force sensitivity, and ΔV_2 is the voltage response of the photodiode on tip II.

Figure 7 shows a full force spectroscopy curve during the pick-and-place manipulation of a microsphere deposited on a glass slide with an ambient temperature of 20 °C and a relative humidity of 38%. The force spectroscopy curve is synthesized from the force responses on tip I and tip II. The

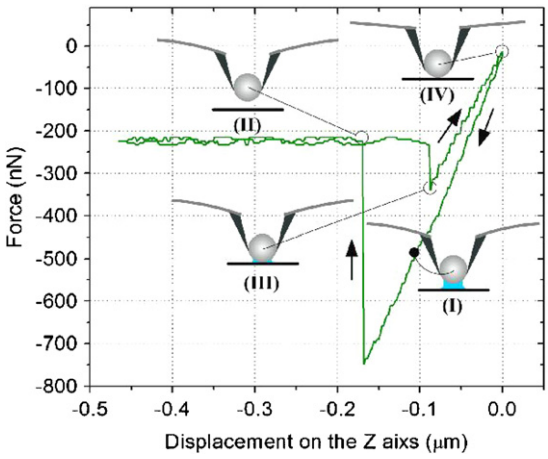

Figure 7. Synthesized normal force responses from both microcantilevers during the pick-and-place manipulation of a microsphere: (I) pick-up, (II) pull-off, (III) snap-in, (IV) contact on the retraction branch.

curve starts from the contact state between the microsphere and the substrate. As the nanostage is moved down to pick up the microsphere, the cantilever is bent, leading to negative forces. During the pick-up, when the nanostage position reaches −170 nm, the microsphere pulls off the substrate with a minimum force of −746 nN. After the pull-off, the force returns to −220 nN, and not to the initial force because of contributions of friction forces between the gripper and the microsphere. Inset I shows that the microsphere slides down to the substrate during the pick-up operation, which leads to bending deformations maintained by the friction on the nanotips, as shown in inset II. During the retracting branch, earlier snap-in occurs at a distance of about 50 nm from the starting point, which indicates that the microsphere slides the same distance during the pick-up operation, as seen in inset III. Further retraction leads to a continued increase in the force response with a higher gradient than that of the pick-up operation until both the nanostage position and the magnitude of the normal force return to the initial grasping state in inset IV. Once such a force spectroscopy curve occurs during the pick-and-place manipulation, a stable grasping as well as a successful releasing operation can be validated.

4. Experimental results and discussion

4.1. Task description

In order to validate 3D automated manipulation capability of the developed 3DMS, nylon microspheres with diameters of 3 μm–4 μm were manipulated to build 3D microstructures in our experiments. The microspheres were deposited on a freshly cleaned glass slide, and then an area of interest for the experiments was selected under an optical microscope with a 20 × lens. figure 8 shows a plan image view of the selected area, which contains more than 24 microspheres; 20 of which separated in a 56 μm square frame are going to be manipulated to build 5 microsphere pyramids labeled by assembly sequences from I to V. Each pyramid is constructed from four microspheres with two layers. The bottom insets

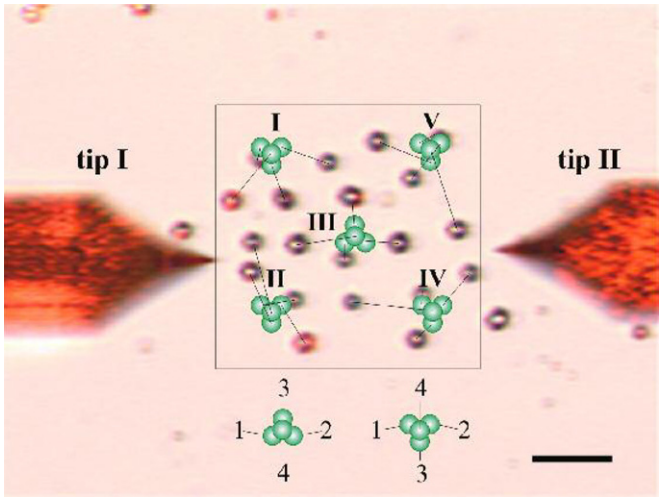

Figure 8. An optical microscope image before the micromanipulation. Twenty microspheres with diameters of 3 μm–4 μm will be manipulated to build five microsphere pyramids (labeled from I to V). The bottom insets show two types of assembly sequences depicted by numbers. The scale bar represents 15 μm.

show two types of assembly sequences, depicted by numbers, for two different arrangements of the pyramids. Tip I and tip II, with a laser spot focused on each cantilever end, are located beside the manipulation area after system initialization, for the convenience of task planning. After task planning, a 3D microassembly task is performed with the sequences predefined from the motion planning to build five micropyramids, shown as schematic structures by green microspheres.

4.2. Manipulation results

Figure 9 shows the 3D micromanipulation process of the micropyramids. Figures 9(*a*) and (*b*) are intercepted when the first layers of pyramids II and VI are assembled, respectively. The image shown in figure 9(*c*) is captured as the first layer of the 5 pyramids has been completed, in which 20 microspheres have been already placed in their reference positions with the pick-and-place operations. Once the first layer is ready, the remaining five microspheres are sequentially picked up and placed on the second-layer reference positions. Figures 9(*d*) and (*e*) describe the transporting process of the 21st and the last microsphere, respectively. The ultimate result is shown in figure 9(*f*). In addition, the assembly result is displayed more distinctly under the microscope with a magnification of 100 ×, as seen in figure 9(*g*).

The whole manipulation process was completed in 16 min excluding the time required for the user to relocate the gripper; so the average manipulation time of each microsphere is about 48 s, which mainly includes about 20 s for microsphere grasping including the processes of grasping point searching and contact detection using amplitude feedback, 10–35 s for microsphere release and the remaining time for transport. The release time for the microspheres on the second layer is much longer than that for the first layer because substantial contact between microspheres is more difficult to achieve

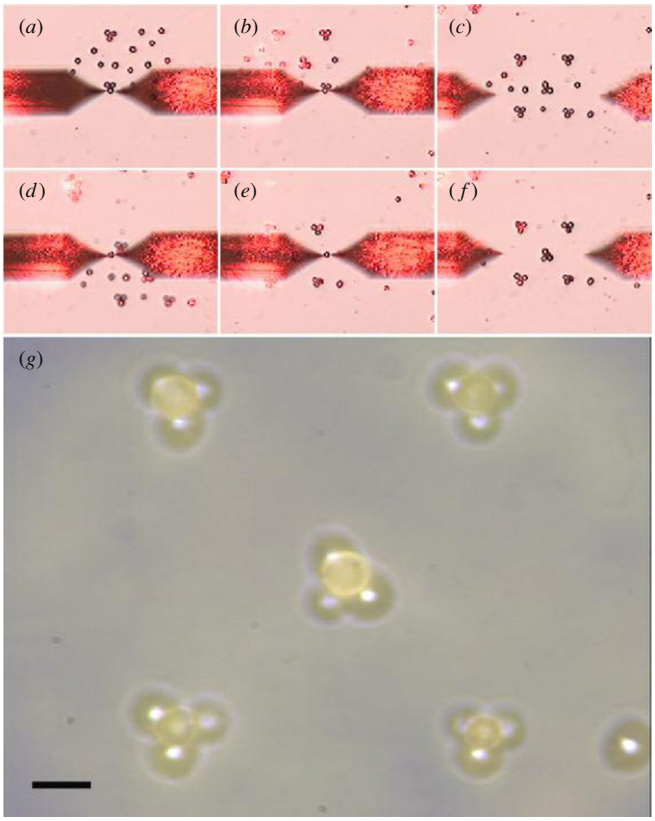

Figure 9. 3D microassembly results of the micropyramids. (*a*)–(*c*) show three images intercepted from the assembly process of the first layer of the micropyramids. (*d*)–(*f*) depict the assembly process of the second layer of the micropyramids. The images (*a*)–(*f*) are captured under magnification of 20×. (*g*) The 3D microassembly results under magnification of 100×. The scale bar represents 5 μm.

than the microsphere–substrate contact, especially the second-layer microspheres on pyramid II and pyramid IV, which have smaller diameters than the supporting microspheres. These two microspheres were successfully released after two release operations. Several aspects of the microassembly can be explained in detail as follows.

As mentioned above, the sharp AFM tip results in tiny adhesion forces between the gripper and the microsphere. However, in order to achieve a reliable release operation, it is first necessary to make certain that the very end of tip I is in contact with the microsphere by keeping a proper distance between the tips and the substrate in the grasping operation. Moreover, it is very important to ensure a full microsphere–substrate contact by waiting for several seconds before opening the nanotip gripper. In addition, the tips should keep dithering in their natural resonance during the whole pick-and-place manipulation procedure, especially in the release process. In order to reduce adhesion forces between the gripper and the microsphere, attributable to the high inertial forces applied to the microsphere [19]. In our experiments, the dithering gripper did not fail once in 40 times of pick-and-place manipulations of the microsphere deposited on the glass slide; in contrast, four microsphere release failures occurred using the non-dithering gripper. By applying schemes or strategies mentioned above, the sticking obstacle is estimated in the experiments.

In addition, note that several interruptions occurred in user's nanotip gripper relocation operations during the whole microassembly of the five micropyramids due to the constraint of the limited nanostage motion range of 50 μm × 50 μm, which is less than the manipulation area of 56 μm × 56 μm. The gripper relocation was completed by moving the microstage and the manual stage for tip I and tip II, respectively. However, the pick-and-place manipulation of each single microsphere is definitely automated.

5. Conclusion

It is well known that the mechanical pick-and-place manipulation at the scale of several microns to the submicron scale is still not well resolved, especially manipulation confined in air. Fortunately, the newly developed 3D micromanipulation system (3DMS) has achieved such a type of pick-and-place micromanipulation using a gripper constructed from two AFM tips. In order to validate the manipulation capability of the 3DMS, microspheres with diameters of 3 μm–4 μm were manipulated in air, and as a result, five 3D micropyramids were constructed with the developed 3DMS. The 3DMS has made the automated 3D micromanipulation and microassembly at the scale of several micrometers in air feasible.

Currently, automated 3D micromanipulation is achieved with microspheres of several micrometers. In the future, we will make efforts to scale manipulation targets down to the submicron scale and ultimately, to the nanoscale, which will require our resolving several issues, and successfully achieving several breakthroughs, such as new strategies or schemes to overcome severe sticking problems at the nanoscale and compensation for nanopositioning errors due to thermal drift, and so on.

Acknowledgment

This work was supported in part by the French National Agency of Research through the NANOROL project.

References

[1] Dechev N, Cleghorn W L and Mills J K 2004 Microassembly of 3-D microstructures using a compliant, passive microgripper *J. Microelectromech. Syst.* **13** 176–89
[2] Xie H, Rong W B and Sun L N 2007 A flexible experimental system for complex microassembly under microscale force and vision-based control *Int. J. Optomechatro.* **1** 80–102
[3] Yang G, Gaines J A and Nelson B J 2003 A supervisory wafer-level 3D microassembly system for hybrid MEMS fabrication *J. Intell. Robot. Syst.* **37** 43–68
[4] Aokil K, Miyazakl H T, Hirayama H, Inoshita K, Baba T, Sakoda K, Shinya N and Aoyagl Y 2003 Microassembly of semiconductor three dimensional photonic crystals *Nat. Mater.* **2** 117–21
[5] Wang W H, Liu X Y, Gelinas D, Brian Ciruna B and Sun Y 2007 A fully automated robotic system for microinjection of zebrafish embryos *Plos ONE* **9** e862
[6] Sun Y and Nelson B J 2002 Biological cell injection using an automated microrobotic system *Int. J. Robot. Res.* **21** 861–8

[7] Lu Z, Chen P C Y, Nam J, Ge R W and Lin W 2007 A micromanipulation system with dynamic force-feedback for automatic batch microinjection *J. Micromech. Microeng.* **17** 314–21
[8] Gauthier M and Piat E 2006 Control of a particular micro-macro positioning system applied to cell micromanipulation *IEEE Trans. Autom. Sci. Eng.* **3** 264–71
[9] Marcy Y, Prost J, Carlier M F and Sykes C 2004 Forces generated during actin-based propulsion: a direct measurement by micromanipulation *Proc. Natl. Acad. Sci. USA* **101** 5992–7
[10] Onal C D and Sitti M 2007 Visual servoing-based autonomous 2-D manipulation of microparticles using a nanoprobe *IEEE Trans. Control Syst. Technol.* **15** 842–52
[11] Nguyen N T, Ho S S and Low C L N 2004 A polymeric microgripper with integrated thermal actuators *J. Micromech. Microeng.* **14** 969–74
[12] Millet O, Bernardoni P, Régnier S, Bidaud P, Tsitsiris E, Collard D and Buchaillot L 2004 Electrostatic actuated micro gripper using an amplification mechanism *Sensors Actuators* **A114** 371–8
[13] Clévy C, Hubert A, Agnus J and Chaillet N 2005 A micromanipulation cell including a tool changer *J. Micromech. Microeng.* **15** S292–S301
[14] Pérez R, Agnus J, Clévy C, Hubert A and Chaillet N 2005 Modeling, fabrication, and validation of a high-performance 2-DoF piezoactuator for micromanipulation *IEEE-ASME Trans. Mechatro.* **10** 161–71
[15] Carrozza M C, Eisinberg A, Menciassi A, Campolo D, Micera S and Dario P 2000 Towards a force-controlled microgripper for assembling biomedical microdevices *J. Micromech. Microeng.* **10** 271–6
[16] Neild A, Oberti S, Beyeler F, Dual J and Nelson B J 2006 A micro-particle positioning technique combining an ultrasonic manipulator and a microgripper *J. Micromech. Microeng.* **16** 1562–71
[17] Walle B L, Gauthier M and Chaillet N 2008 Principle of a submerged freeze gripper for microassembly *IEEE Trans. Robot.* **24** 897–902
[18] Kim K Y, Liu X Y, Zhang Y and Sun Y 2008 Nanonewton force-controlled manipulation of biological cells using a monolithic MEMS microgripper with two-axis force feedback *J. Micromech. Microeng.* **18** 055013
[19] Haliyo D S, Dionnet F and Régnier S 2006 Controlled rolling of micro-objects for autonomous manipulation *J. Micromechatro.* **3** 75–101
[20] Driesen W, Varidel T, Régnier S and Breguet J M 2005 Micromanipulation by adhesion with two collaborating mobile micro robots *J. Micromech. Microeng.* **15** S259–67
[21] Park I-Y, Sung S-Y, Lee J-H and Lee Y-G 2007 Manufacturing micro-scale structures by an optical tweezers system controlled by five finger tips *J. Micromech. Microeng.* **17** N82–9
[22] Sitti M 1999 Teleoperated 2-D micro/nanomanipulation using an atomic force microscope *PhD Thesis*, University of Tokyo, Japan, http://www.cs.cmu.edu/˜msitti/pub.html
[23] Menciassi A, Eisinberg A, Izzo I and Dario P 2004 From 'macro' to 'micro' manipulation: models and experiments *IEEE-ASME Trans. Mechatro.* **9** 311–20
[24] Lambert P and Régnier S 2006 Surface and contact forces models within the framework of microassembly *J. Micromechatro.* **3** 123–57
[25] Sitti M 2007 Microscale and nanoscale robotics systems-characteristics, state of the art, and grand challenges *IEEE Robot. Autom. Mag.* **14** 53–60
[26] Xie H, Rong W B and Sun L N 2007 Construction and evaluation of a wavelet-based focus measure for microscopy imaging *Microsc. Res. Tech.* **70** 987–95
[27] Liu X Y, Wang W H and Sun Y 2007 Dynamic evaluation of autofocusing for automated microscopic analysis of blood smear and pap smear *J. Microsc.* **227** 15–223
[28] Xie H, Rong W B, Sun L N and Chen W 2006 Image fusion and 3-D surface reconstruction of microparts using complex valued wavelet transforms *IEEE Intl Conf. Image process (Atlanta, GA)* pp 2137–40
[29] Xie H, Vitard J, Haliyo S and Régnier S 2008 Optical lever calibration in atomic force microscope with a mechanical lever *Rev. Sci. Instrum.* **79** 096101
[30] Xie H, Rakotondrabe M and Régnier S 2009 Characterizing piezoscanner hysteresis and creep using optical levers and a reference nanopositioning stage *Rev. Sci. Instrum.* **80** 046102
[31] Vögeli B and Känel H von 2000 AFM-study of sticking effects for microparts handling *Wear* **238** 20–4
[32] Varenberg M, Etsion I and Halperin G 2003 An improved wedge calibration method for lateral force in atomic force microscopy *Rev. Sci. Instrum.* **74** 3362–7
[33] Xie H, Vitard J, Haliyo S and Régnier S 2008 Enhanced accuracy of force application for AFM nanomanipulation using nonlinear calibration of optical Levers *IEEE Sensors J* **8** 1478–85